LBL-22608

Lawrence Berkeley Laboratory
UNIVERSITY OF CALIFORNIA

Materials & Molecular Research Division

Presented at the International School on Electronic Band Structure, Kanpur, India, October 20-November 8, 1986; and to be published in **Lecture Notes on International School on Electronic Band Structure and Its Applications,** M. Yussouff, Ed., Springer-Verlag 1987

ALLOY PHASE STABILITY

D. de Fontaine

November 1986

Prepared for the U.S. Department of Energy under Contract DE-AC03-76SF00098

DISCLAIMER

LBL-22608

ALLOY PHASE STABILITY

Didier de Fontaine
Materials and Molecular Research Division
Lawrence Berkeley Laboratory
and
Department of Materials Science and Mineral Engineering
University of California
Berkeley, California 94720 USA

October 1986

This work was supported by the Director, Office of Energy Research, Office of Basic Energy Sciences, Materials Sciences Division of the U.S. Department of Energy under Contract No. DE-AC03-76SF00098.

To be published in "Lecture Notes on International School on Electronic Band Structure and its Applications" held at IIT Kanpur, India, Oct. 1986, M. Yussouff, Ed., Springer-Verlag 1987.

ALLOY PHASE STABILITY

Didier de Fontaine
Dept. of Materials Science
and Mineral Engineering
University of California
Berkeley, CA 94720/USA

1. Introduction

Pure elements, metals for example, can exist in different phases: gas, liquid, solids of various crystal structure. In general, as the temperature is lowered, phases of high disorder (fluids) are replaced by phases of greater order (crystals). In alloys, *chemical order* (or disorder) can combine with the *geometrical order* (or disorder) mentioned above, to produce a wide variety of phases found at equilibrium in certain ranges of composition and temperature (or pressure). In addition to phases found in equilibrium phase diagrams, others, with free energy only slightly different from those of the equilibrium ones, can be made to appear under certain circumstances (rapid cooling, irradiation, and so on). The problem of phase stability in alloys is thus a very complex one which is inherently non-local; i.e. at fixed composition, if is not sufficient to ask which phase has the lowest free energy, it is also necessary to compare the stabilty of a given phase to that of a the mixture of two or more phases of different compositions (but with fixed average composition).

The phase stability problem will be examined here for the case of *prototype* alloys containing two types of atoms, A and B, say. Only crystalline structures will be envisaged, and very simple ones at that: those based on the fcc and bcc lattices. Furthermore, atomic displacements from ideal lattice sites will not be considered, hence neither elastic distortions nor vibrational entropy effects will be taken into account. Phase stability analysis will thus be confined to comparing the free energies of Ising models on different rigid lattice frameworks.

These simplifications are necessary, at least at this stage of the investigation, because of the considerable complexity of the problem: indeed, we wish, ultimately, to perform *first principles* calculations of alloy free energies by performing both Quantum Mechanical and Statistical Thermodynamical calculations with the least possible number of empirical or adjustable parameters. This calls for electronic band structure calculations of disordered systems by coherent potential approximation (CPA) techniques. In principle, it is possible to perform *ab initio* calculations for each alloy composition by KKR-CPA methods,[1] but, at this stage, it seems preferable to consider the properties and electronic structure of the pure elements A and B as given (as determined by very accurate band structure calculations), and to obtain the alloy states as interpolations between those of the

pure elements. Therefore, a simple tight binding (TB) approximation will be used.

As for the all-important configurational entropy contribution, it will be approximated by the cluster variation method (CVM), which has proved to be highly reliable,[2] unlike the Bragg Williams approximation, which can fail rather badly, especially in the case of fcc ordered superstructures.

The outline of the present lecture notes follows roughly that of some previous papers by the author:[3-5] State of Order (Sect. 2), Cluster Variation Method (Sect.3), Internal Energy (Sect. 4), Quantum Mechanical Interpolation (Sect.5), Ground States of order (Sect. 6), Construction of Phase Diagrams (Sect. 7), Prototype Diagrams (Sect. 8), Conclusion (Sect. 9). Much progress has been made since the earlier papers were written, however, as will be summarized below.

2. State of Order

Calculations of properties of pure elements and stoichiometric compounds has progressed considerably in recent years, but it is clear that alloys (mixtures of one or more elements) present additional difficulties. Pure crystals or compounds can be uniquely described by their unit cells, and completely disordered solid solutions can be described by specifying the average lattice and the average composition. For phase equilibrium calculations, however, it is essential to consider *states of partial order*: arbitrary degrees of long-range order (LRO), with short-range order (SRO) present as well.

In 1951, Kikuchi proposed the Cluster Variation Method[6] (CVM) which, initially, was regarded as a heuristic method for improving the traditional mean field approximations of statistical mechanics, such as the Bragg-Williams (BW) method. Lately, it has been shown[7] that the CVM, in a new formulation, actually provides a completely general and optimal way of describing partial compositional order, the basic idea being to represent partially ordered systems by sampling configuration space by means of small clusters of crystal lattice sites. In its latest development, the theory makes use of the decomposition of functions of configuration in terms of a complete set of orthonormal functions. This method will be summarized here, following the paper by Sanchez, Ducastelle and Gratias[7] (SDG).

In SDG, multicomponent systems were considered. Here, for simplicity, only binary systems will be treated. Each lattice site (p) can then be occupied by either an A or a B atom, with corresponding "spin" variable σ_p=+1 or -1. The complete crystal, of N sites, has instantaneous configuration fully specified by the vector $\sigma=\{\sigma_1,\sigma_2,\ldots\sigma_N\}$. The scalar product of two functions of configuration, $f(\sigma)$ and $g(\sigma)$, is defined as

$$\langle f,g\rangle = \rho_N^{\bullet}\ \mathrm{Tr}^{(N)} f\cdot g \qquad (1)$$

where the "trace" operation is defined as a sum over all configurations

$$Tr^{(N)} = \sum_{\sigma_1=\pm 1} \sum_{\sigma_2=\pm 1} \cdots \sum_{\sigma_N=\pm 1} \qquad (2)$$

with normalization

$$\rho_N^\circ = 2^{-N} \quad .$$

The scalar product definition (1) allows the construction of a complete orthonormal set (CONS) of functions. For a single lattice point, the set of functions is simply

$$\Gamma(\sigma_p) = \{\Gamma_0, \Gamma_1\} = \{1, \sigma_p\} \qquad (3)$$

such that

$$\langle \Gamma_i(\sigma_p), \Gamma_j(\sigma_p) \rangle = \delta_{ij} \qquad (4)$$

where the Kronecker delta is unity if i=j, zero otherwise. Now form the direct product, over all N lattice sites,

$$\Gamma(\sigma_1) \times \Gamma(\sigma_2) \times \ \ldots \ \times \Gamma(\sigma_N) = \Phi \ . \qquad (5)$$

By (5), each function of the set Φ, except $\Phi_0=1$, is itself a product

$$\Phi_\alpha = \sigma_{p_1} \sigma_{p_2} \ldots \sigma_{p_n}$$

over the cluster $\sigma=\{p_1, p_2, \ldots p_n\}$ of n points.

From (1) and (4) we then have

$$\langle \Phi_\alpha, \Phi_\beta \rangle = \delta_{\alpha\beta} \qquad (6)$$

and the closure relation

$$\rho_N^\circ \sum_\beta \Phi_\beta(\sigma) \Phi_\beta(\sigma') = \delta_{\sigma,\sigma'} \quad . \qquad (7)$$

Hence, by (4) and (7) the set Φ is a CONS. It is convenient to treat separately the configuration independent function $\Phi_0=1$. Then any function may be expanded as

$$g(\sigma) = g_0 + \sum_\alpha g_\alpha \Phi_\alpha(\sigma) \qquad (8)$$

with

$$g_0 = \langle 1, g \rangle \quad , \quad g_\alpha = \langle \Phi_\alpha, g \rangle \quad . \qquad (9)$$

For example, the Ising Hamiltonian may be expanded in terms of *cluster fucntions* Φ_α as follows

$$\mathcal{H} = \sum_\alpha \omega_\alpha V_\alpha \Phi_\alpha \quad , \qquad (10)$$

the V_α being *cluster interactions* given by

$$\omega_\alpha V_\alpha = \langle \Phi_\alpha, \mathcal{H} \rangle \quad , \qquad (11)$$

where the ω_α are numerical factors which may be introduced for convenience in comparing with other treatments.

To evaluate averages, it is necessary to define a configuration density thus

$$\rho(\sigma) = Z^{-1}\ e^{-\mathcal{H}/k_B T} \tag{12}$$

with partition function

$$Z = \mathrm{Tr}^{(N)}\ e^{-\mathcal{H}/k_B T} \tag{13}$$

where $k_B T$ has its usual meaning. The density can also be expanded in orthonormal functions

$$\rho(\sigma) = \rho_N^{\circ}\ [1 + \sum_{\alpha} \Phi_\alpha(\sigma)\xi_\alpha] \tag{14}$$

where ξ_α is a *multiplet correlation function* for cluster α, defined as the average value of the product of σ variables over the cluster α

$$\xi_\alpha = \langle \Phi_\alpha, \rho \rangle = \rho_N^{\circ}\ \langle \Phi_\alpha \rangle \tag{15}$$

It is also useful to consider *reduced densities* obtained by performing the partial trace

$$\rho_\beta = \mathrm{Tr}^{(N-\beta)}\rho \quad , \tag{16}$$

i.e. by summing over all configurations except that, σ_β, of the n-point cluster β envisaged. The partial trace operating on Φ_α in (14) equals $(1/\rho_\beta^{\circ})\Phi_\alpha$ if α is contained in β ($\alpha c \beta$) and zero otherwise, where $1/\rho_\beta^{\circ} = 2^n$. The reduced density can be regarded as the expectation value, in an ensemble of systems, of the cluster β having configuration σ_β. Thus, $\rho_p(\sigma_p)$ is simply the average concentration of A (σ_p=+1) or B (σ_p=-1) atoms, at site p, over the ensemble. If all lattice points p are equivalent, then ρ_p is the crystal average. If long-range order is present, distinct sub-lattices must be defined, and averages taken only over all points of a given sublattice, p_1, say. By combining Eqs. (14) and (16) we then have, for cluster concentrations, or reduced densities, expressed in terms of correlations functions,

$$\rho_\beta(\sigma_\beta) = \rho_\beta^{\circ}[1 + \sum_{\alpha c \beta} \Phi_\alpha(\sigma_\beta)\xi_\alpha] \quad . \tag{17}$$

This important formula was first derived by Sanchez[8]. The notion of partial trace was introduced into the CVM by Morita.[9] In practice, it is convenient to group all ξ_α which are identical because of the symmetry of the crystal structure. Equations (14) or (17) then take on a slightly different form, with appropriate sums of Φ_α functions being regarded as elements of the so-called *configuration matrix*. The crystallography of the problem is thus introduced into the statistical formulation by means of this matrix.

3. Cluster Variation Method

The energy and configurational entropy can be written as, respectively,

$$E[\rho] = \mathrm{Tr}^{(N)}\ \rho\mathcal{H} \tag{18}$$

and

$$S[\rho] = -k_B \, Tr^{(N)} \rho \, \ell n \, \rho \quad . \tag{19}$$

The free energy is then given by

$$F[\rho] = Tr^{(N)} \, \rho[\mathcal{H} + k_B T \, \ell n \, \rho] \quad . \tag{20}$$

E, S and F are to be regarded as functionals in $\rho(\sigma)$, and will take on their equilibrium (expectation) values if ρ corresponds to the correct equilibrium distribution of configurations. In traditional variational treatments, $F[\rho]$ is minimized with respect to ρ subject to the constraint $Tr\rho=1$. It was shown by SDG[7], however, that the equilibrium free energy could be obtained by a purely algebraic procedure, as will now be demonstrated. In a sense, the "Variation" has now been taken out of the Cluster Variation Model. It is, of course, impossible to consider the full density function $\rho(\sigma)$ over all configurations on all lattice sites. Hence, some method must be devised for handling only a small number of configurations. In the CVM, this is accomplished by considering configurations over a few small clusters, up to some maximum-size cluster(s). Usually, the larger the clusters retained, the better will be the approximation to the free energy.

In the energy expression, the approximation consists of neglecting interaction energies V_α in Eq. (10) for all clusters not contained in the maximal cluster(s) (see justification, later on). The same simple procedure will not do for the entropy expression, however: the $\ell n \, \rho$ term cannot be written as a truncated sum of partial densities of the type (16), as no convergence is expected. Instead, following Morita[9], we define new functions $\tilde{\rho}_\beta$ by writing successively

$$\rho_1 = \tilde{\rho}_1 \quad , \quad \rho_{12} = \tilde{\rho}_1 \tilde{\rho}_2 \tilde{\rho}_{12} \quad , \quad \cdots \quad \rho_\alpha = \prod_{\beta \subset \alpha} \tilde{\rho}_\beta \quad , \quad \cdots$$

with, finally

$$\rho = \prod_\alpha \tilde{\rho}_\alpha \tag{21}$$

The CVM approximation consists in truncating the product (21), by assuming that the cumulant corrections $\tilde{\rho}_\gamma$ for γ not contained in the maximal cluster(s) are equal to unity. Hence,

$$\ell n \, \rho \cong \sum_\beta{}' \, \ell n \, \tilde{\rho}_\beta \tag{22}$$

the accent on the summation denoting a truncated sum. It is now necessary to relate the $\ell n \, \tilde{\rho}_\beta$ ($=\Omega_\beta$, say) to $\ell n \, \rho_\alpha$ ($=\Lambda_\alpha$, say) which can be done by procedures already developed by Barker[10] and Hijmans and de Boer[11]. To this end, we write Eq. (22) as a sum over the Λ_α times some coefficients a_α, the latter being determined only by geometrical considerations:

$$\sum_\beta{}' \, \Omega_\beta = \sum_\alpha{}' \, a_\alpha \Lambda_\alpha = \Sigma' \, a_\alpha \sum_{\beta \subset \alpha} \Omega_\beta = \sum_\beta{}' \, \Big(\sum_{\alpha \supset \beta} a_\alpha \Big) \, \Omega_\beta \quad . \tag{23}$$

Therefore,

$$\sum_{\alpha \supset \beta} a_\alpha = 1 \quad , \tag{24}$$

there being a separate Eq. (24) for each subcluster α contained in the set of maximal clusters. Thus, the a_α can be determined uniquely by recursion.

We have therefore derived an important expression

$$\ell n\ \rho = \sum_\alpha{}' a_\alpha\ \ell n\ \rho_\alpha \tag{25}$$

whereby the logarithm of the density function is approximated by a weighted sum of reduced densities, i.e. cluster concentrations. By taking the logarithm of both sides of Eq. (12) we have

$$\ell n\ \rho = -\ell n\ Z - \frac{\mathcal{H}}{k_B T}$$

or, using (25),

$$k_B T \sum_\alpha{}' a_\alpha\ \ell n\ \rho_\alpha = (-k_B T\ \ell n\ Z)\Phi_o - \sum_\beta \omega_\beta V_\beta \Phi_\beta \quad .$$

By the properties of the CONS we therefore have, as in Eq. (9):

$$-k_B T\ \ell n\ Z = \langle 1,\ k_B T \sum_\alpha{}' a_\alpha\ \ell n\ \rho_\alpha \rangle \tag{26}$$

and

$$-\omega_\beta V_\beta = \langle \Phi_\beta,\ k_B T \sum_\alpha{}' a_\alpha\ \ell n\ \rho_\alpha \rangle \quad . \tag{27}$$

the latter equation can be rewritten as

$$\omega_\beta V_\beta = -\sum_{\alpha \supset \beta} a_\alpha\ \rho_\alpha{}^o\ \mathrm{Tr}^{(\alpha)}\ \Phi_\beta(\sigma_\alpha)\ \ell n\ \rho_\alpha \tag{28}$$

which is exactly the result which would have been obtained by direct minimization of the free energy with respect to the correlation functions ξ_β. In the Eqs. (28), the ρ_α must be replaced by their expressions in terms of the independent variables ξ_β. There results a set of non-linear equations in as many unknowns as there are maximal clusters and their distinct subclusters. Solving this set of equations by numerical techniques constitutes a major difficulty of the CVM, hence, in practice, clusters must be kept small and few in number.

By a well-known result of statistical mechanics, Eq. (26) gives directly the equilibrium free energy:

$$F = k_B T \sum_\alpha a_\alpha\ \mathrm{Tr}^{(\alpha)}\ \ell n\ \rho_\alpha \quad . \tag{29}$$

The free energy functional itself is, from Eqs. (20), (10), (15) and (25),

$$F[\rho] = \sum_\beta \omega_\beta V_\beta \xi_\beta + k_B T \sum_\alpha a_\alpha\ \mathrm{Tr}^{(\alpha)}\ \rho_\alpha\ \ell n\ \rho_\alpha \tag{30}$$

which is the classical CVM expression for the free energy. Note that the two sums in Eq. (30) need not run over the same clusters; it is only required that the entropy sum contain the maximal cluster(s), and the energy sum include only

clusters contained in the maximal one(s). Of course, some of the a_α subclusters may vanish, as explained by SDG.[7]

4. Internal Energy

In order to calculate phase diagrams, it is not sufficient to treat Ising models alone: it is required to evaluate cohesive energies of various phases, in various states of order, referred to the same reference energy, for instance the energy of an infinitely dilute gas of pure A and pure B atoms, respectively denoted E_A^∞ and E_B^∞ in Fig. 1. E_A^α and E_B^α are then the cohesive energies of pure A and B in the α phase (fcc lattice, say) and E_A^β and E_B^β are the corresponding cohesive energies in the β phase (bcc, say). Linear interpolations between those pure states are indicated by dashed straight lines. Actually, the cohesive energy E_{dis} of random mixtures of A and B, in α or β (denoted E_o^α and E_o^β in Fig. 1), as a function of concentration c of B atoms, will differ from the linear interpolation by amount ΔE_{dis} (denoted E_M^α or ΔE_M^β in Fig. 1), the energy of completely random mixing.

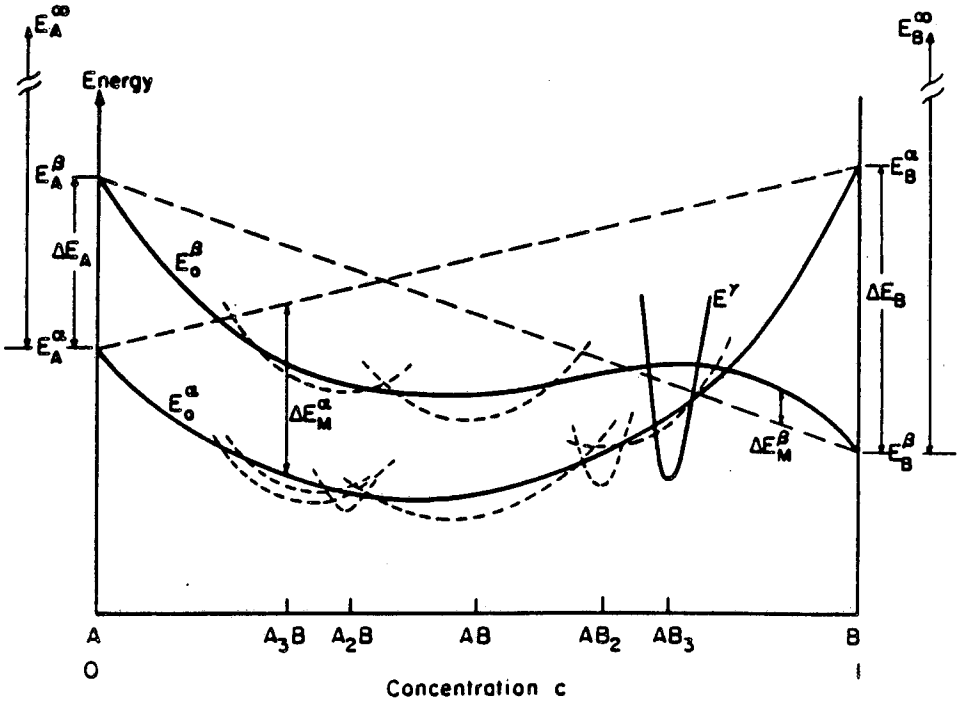

Fig. 1. Cohesive energies E_o^α and E_o^β of completely disordered α and β phases and of a possible compound γ (full curves), and schematic representation of energies of (partially) ordered superstructures (dashed curves) as a function of concentration c.

Going beyond the simple Ising Hamiltonian (10), it is possible to use the concepts derived in Sects. 2 and 3 to obtain formal expressions for the physical energy parameters required, namely E_{dis} and the V_α, defined in (10) and (11). To that end, let $E(\sigma)$ denote the cohesive energy of a particular configuration (σ), on a given lattice $(\alpha,\beta,\ldots)$. The expectation value of E, for distribution ρ, will be

$$\langle E\rangle = \mathrm{Tr}^{(N)}\ \rho(\sigma)\ E(\sigma) \tag{31}$$

Inserting expression (14) for the density ρ into (31) then yields

$$\langle E\rangle = E_o + \sum_\alpha E_\alpha\ \xi_\alpha \tag{32}$$

with

$$E_o = \rho_N^*\ \mathrm{Tr}^{(N)}\ E(\sigma) \tag{33}$$

and

$$E_\alpha = \langle \phi_\alpha, E\rangle = \rho_N^*\ \mathrm{Tr}^{(N)}\ \phi_\alpha(\sigma)\ E(\sigma) \tag{34}$$

Note that, in this *grand canonical averaging*, because of the Trace operation, the energy E_o and the effective cluster interactions E_α are not only configuration independent but even concentration independent.

Let us rewrite (34) explicitely for the case of pair interactions E_r, where r denotes the spacing between lattice points p and q of the pair:

$$E_r \equiv E_{pq} = \frac{1}{2^2} \sum_{\sigma_p=\pm 1} \sum_{\sigma_q=\pm 1} \sigma_p\sigma_q\ \frac{1}{2^{N-2}}\ \mathrm{Tr}^{(N-2)}\ E(\sigma) \tag{35}$$

where the trace operation is carried out everywhere except at p and q. From Eq. (35) follows

$$E_r = \omega_r V_r = \frac{1}{4}\ (V_{AA} - V_{AB} - V_{BA} + V_{BB}) \quad , \tag{36}$$

where V_{ij} (i,j=A,B) represents the energy of the r^{th} (i,j) pair embedded in an artificial medium in which all configurations are equally represented. Through Eq. (35), the pair interactions (or more general cluster interactions E_α) may be related to the V_α used in the Ising model of the previous sections.

Unfortunately, Eqs. (34) or (35) cannot be used to calculate the cluster interactions since the configuration energies $E(\sigma)$ are, of course, not known. Hence, a more direct method of computation for the E_α is required. It has been argued[12,13] that the proper way to calculate effective cluster interactions is by means of a perturbation expansion of a disordered medium of specified concentration c. It appears that the expansion is much more rapidly convergent if the states of (partial) order (dashed curves in Fig. 1) are considered as perturbations of the disordered states (full curves) rather than as perturbations of the pure states or their linear interpolations (dashed straight lines in Fig. 1). Quantum mechanical techniques suitable for performing such calculations will be outlined in the next Section. For now, let us merely show how Eqs. (31) to (35) must be modified

formally in order to obtain disordered state energies and concentration dependent cluster interactions.

In a sample containing a large number N of atoms, it is expected that, at equilibrium, the concentration c of the systems in a grand canonical ensemble will hardly ever depart significantly from the equilibrium concentration c^*. In other words, the density function $\rho(\sigma)$ will be very sharply peaked about configurations having average concentration c^*. Hence, in Eq. (31), it is practically equivalent to sum only over those configurations $\{\sigma^*\}$, all of which have concentration σ^*:

$$\langle E \rangle \cong \mathrm{Tr}^{(N)}\ \rho(\sigma^*)\ E(\sigma^*) \tag{37}$$

where the superscript $(^*)$ denotes *canonical averaging*, as it were. We now have

$$\langle E \rangle = E_o^* + \sum_\alpha E_\alpha^*\ \xi_\alpha \tag{38}$$

with

$$E_o^* = \rho_N^*\ \mathrm{Tr}^{(N)}\ E(\sigma^*) \tag{39}$$

and

$$E_\alpha^* = \rho_N^*\ \mathrm{Tr}^{(N)}\ \Phi_\alpha(\sigma^*)\ E(\sigma^*) \tag{40}$$

The total number of configurations having fixed number (N_A, N_B) of A and B atoms is

$$M = \frac{N!}{N_A!N_B!} \tag{41}$$

so that the energy of the completely random state of concentration $c^*=N_B/(N_A+N_B)$ is, by Eq. (38),

$$E_{dis} = \frac{1}{M}\ \mathrm{Tr}^{(N)}\ E(\sigma^*) = E_o^* + \sum_\alpha E_\alpha^*\ \xi_\alpha^R \tag{42}$$

where ξ_α^R denote multiplet correlation functions in the fully disordered state. It is now apparent that the disordered energy E_{dis} and the cluster interactions E_α^* are concentration dependent since, in Eqs. (40) and (42), the Trace operation samples different configurations at each concentration c.

The term E_o^* may be eliminated from Eq. (38) by means of Eq. (42):

$$\langle E \rangle = E_{dis} + E_{ord} \tag{43}$$

where the disordered state energy E_{dis} is the energy of the completely disordered medium, in a given crystal structure, calculated in a single-site coherent potential approximation (CPA), for instance, and E_{ord} is given by

$$E_{ord} = \sum_\alpha{}' E_\alpha^*\ \delta\xi_\alpha \tag{44}$$

where

$$\delta\xi_\alpha = \xi_\alpha - (\xi_1)^n \quad , \tag{45}$$

since the correlation function, in the fully disordered state, for an α cluster of n

points is practically equal to n^{th} power of the point correlation function $\xi_1=c_A-c_B=1-2c$. The accent on the summation in Eq. (44) indicates that, because of Eq. (45), the point clusters are not included in the sum. Equations (43) to (45) were given previously by Sigli and Sanchez[14]. The E_α, or V_α in the notation of previous Sections, must now be calculated. As will be shown in the next Section, this can be accomplished by perturbing the single site CPA according to the so-called Generalized Perturbation Method (GPM)[12,13]. Alternately, the Embedded Cluster Method[15] may be used since, by Eq. (40), each cluster interaction V_{ij} in Eq. (36), rewritten for canonical averaging, as in Eq. (40), represents the energy of cluster α embedded in a medium of random configuration of concentration c.

The derivations given above may explain formally why pair interactions E_r, for large spacing r, tend to become small in magnitude: at large spacing in a random medium, V_{ij} is approximately given by the sum of point energies $V_i + V_j$, hence the linear combination $V_{AA} + V_{BB} - 2V_{AB}$ will tend to vanish.

To complete the calculation of the internal energy, E_{ord} must be evaluated, which requires, in addition to the E°_α, knowledge of the equilibrium correlation functions ξ_α. These must be obtained by minimizing the free energy, at given temperature and concentration, by solving the system of algebraic equations (28). In summary, then, E°_{dis} and E°_α (or V_α) can all be calculated by Quantum Mechanical methods at absolute zero of temperature. The ξ_α are calculated by the CVM with temperature independent parameters. Hence, the procedure described here achieves a very convenient decoupling of the Quantum and Statistical Mechanical computations.

5. Quantum Mechanical Interpolation

The difficult problem remains of calculating E_{dis} and the effective cluster interactions E_α. It has been shown[16] that cluster interactions are generally smaller in magnitude than effective pair interactions (EPI), so that only the latter will be retained in the present analysis. The EPI, defined formally by Eq. (36), will be calculated in the Generalized Perturbation Method (GPM)[12,13] applied to a given Quantum Mechanical Model. Some recent progress has been made in implementing the GPM onto the KKR-CPA[17] but thus far, most results have been obtained in the tight binding (TB) approximation.

The TB scheme does not really qualify as a true first principles calculation, but as an interpolation method in the following sense: suppose that very accurate electronic band structure calculations have been performed on the pure elements A and B in the same crystal structure. What then may we deduce for the band structure, in particular the electronic density of states (DOS), n(E), for the random mixture of A and B atoms on the same lattice, as a function of concentration c?

To simplify matters, consider only paramagnetic transition metal elements and

assume that properties of interest (cohesive energy, EPI) are primarily dependent on d-electrons. Hydridization with the s band will thus be neglected. Under those conditions, the wave functions can be expanded in linear combinations of atomic d-orbitals (LCAO), with atomic wave functions denoted $|i\lambda\rangle$, considered members of a CONS, with index i indicating the atomic site and λ the atomic d-orbital. The tight binding Hamiltonian for the pure elements may thus be written

$$H = \sum_i \varepsilon_i |i\lambda\rangle\langle i\lambda| + \sum_{i \neq j} \sum_{\lambda,\mu} \beta_{ij}^{\lambda\mu} |i\lambda\rangle\langle j\mu| \quad , \tag{46}$$

where ε_i is ε_A or ε_B depending on which metal is considered and where $\beta_{ij}^{\lambda\mu}$ are so-called hopping integrals. The energy levels ε_i will be taken as the centers of gravity of the d band of the corresponding pure metal. The hopping integrals connect neighboring sites i and j but cannot be readily evaluated by matrix element integrals, although theory indicates that the magnitude of the β's should decrease as the distance between atomic sites increases. The Slater and Koster method of interpolation is therefore generally used: the β's are considered as adjustable parameters whose values are optimized so as to fit the calculated band structures as closely as possible. Actually, the hopping integrals depend on a smaller number of parameters, the molecular ortibal-like parameters ddσ, ddπ and ddδ[18]. Hence, in this first interpolation step, the electronic properties of pure A and pure B are regarded as being determined entirely by a small set of parameters, and by the number of d electrons per atom, N_A or N_B.

The one-electron energy is given by

$$E_{1e} = \int_{-\infty}^{E_F} n(E)\, E\, dE \tag{47}$$

where E_F is the Fermi energy and where the electronic density of states n(E) (for d electrons) can be computed in the usual manner by taking the limit of the imaginary part of the trace of the pure element Green's function, given formally by

$$G(z) = (z-H)^{-1} \quad . \tag{48}$$

In the present study, the Green's function was calculated by the recursion method[19,20]. The computational procedure used to derive the results to be reported here is explained elsewhere[21,22]. In a recent study,[23] Sigli has proposed an approximate scheme for correcting the one-electron energy (47) for the effects of electron-electron and ion-ion interactions. These effects will not be taken into account here.

In the alloy case, ε_i and $\beta_{ij}^{\lambda\mu}$ in Eq. (46) become random parameters since, *a priori*, it is not known which atom, A or B, occupies sites i, j, etc... It thus becomes imperative to adopt an averaging procedure. Thus far, it has not proved feasible to use a CVM-like scheme, as given in Sect. 2, in the quantum mechanical context. Thus, a zeroth order mean field approximation is used, the coherent potential approximation (CPA). In the single site CPA, parameters ε_i are replaced by an average energy dependent potential σ and the hopping integrals are assumed to

be independent of the nature of the atoms at i and j. Then, let the Green's operator corresponding to that new Hamiltonian be denoted by $\tilde{G}(z-\sigma)$. The potential σ is determined self consistently by the condition on the scattering operators[24]

$$\langle t \rangle = c_A t_A + c_B t_B \tag{49}$$

where

$$t_i = \frac{\Delta\varepsilon_i}{1 - \Delta\varepsilon_i G_{oo}(E-\sigma)} \quad , \quad \Delta\varepsilon_i = \varepsilon_i - \sigma \tag{50}$$

with

$$\tilde{G}_{oo}(z) = \frac{1}{5} \sum_{\lambda} \langle 0\lambda | \tilde{G}(z) | 0\lambda \rangle \quad . \tag{51}$$

Iteration of (49) and (50) determines σ self-consistently. The diagonal elements of the Green's function are determined by the recursion method, as explained above. To calculate the EPI by the GPM, off-diagonal elements

$$\tilde{G}^{\lambda\mu}_{ij} = \langle i\lambda | \tilde{G}(z-\sigma) | j\mu \rangle \tag{52}$$

are also required; these can be obtained, however, by combining appropriate diagonal elements. Finally, the EPI are given by the GPM formula[12,13]

$$V_r \equiv V_{ij} = -\frac{1}{2\pi} \mathrm{Im} \int_{-\infty}^{E_F} dE \, (t_A - t_B)^2 \sum_{\lambda,\mu}{}' \tilde{G}^{\lambda\mu}_{ij}(E-\sigma) \quad . \tag{53}$$

The CPA thus provides the required compositional interpolation between pure A and pure B, on the same lattice (α, say). If another crystal structure were required, the whole calculation would be repeated, including the hopping integral fits for the new lattice (β, say). Of course, pure A and/or pure B may well be metastable on either or both α and β lattice. It is clear that the Green's function $\tilde{G}(z-\sigma)$ is concentration dependent through its dependence on σ, which itself depends on average concentration (though not on SRO), by Eqs. (49) and (50). Therefore, the energy of the purely disordered state, E_{dis}, calculated from Eq. (47) with n(E) obtained from $\tilde{G}$ of the CPA medium, must also be concentration dependent. Furthermore, the Fermi energy E_F depends on the average d-band filling

$$\bar{N}_d = N_A c_A + N_B c_B \tag{54}$$

For the same reason, then, the EPI V_r (recall that the index r denotes the |i-j| distance) also depend on concentration. It is precisely because the GPM appears to be, at present, the preferred method of calculating ordering energies, that the original CVM formulation, with concentration independent E_α interactions, had to be replaced by concentration dependent ones, E^*_α. The V_r of Eq. (53) are thus the EPI defined by Eq. (36), but calculated formally according to the "canonical" averaging described in the previous Section.

In addition to their dependence on hopping integral parameters, the EPI also depend on the d-band filling $\bar{N}_d$ through E_F, as mentioned, and on the levels ε_A and ε_B through Eq. (50), more properly on the normalized energy level difference, or

$$\delta_d = \frac{\varepsilon_B - \varepsilon_A}{\bar{w}} \qquad (55)$$

where $\bar{w}$ is the average of the half d-band width of the elements. The EPI should also depend on non-diagonal disorder

$$\delta_{nd} = \frac{w_B - w_A}{\bar{w}} \quad , \qquad (56)$$

but that dependence was neglected in preliminary studies reported upon here[21,22]. If "canonical" Slater-Koster parameters are used, then $\bar{w}$ turns out to be a normalization factor which fixes the energy scale, so that the EPI have the following functional dependence

$$V_r = \bar{W}\ f(c,\bar{N}_d,\delta_d,\delta_{nd}) \quad . \qquad (57)$$

The EPI thus depend only on the average alloy concentration c and on electronic parameters of the pure elements A and B.

6. Ground States of Order

The consequences of this functional dependence of the EPI on the various alloy system parameters have been investigated in detail (see Ref. 25, for example, and bibliography cited therein). Particularly interesting and quite accurate predictions have been made concerning *ground states of order*. By this expression is meant those ordered configurations of A and B atoms on the sites of a given fixed lattice which minimize the energy E, at zero absolute, given the stoichiometry c and values of pair interactions V_r.

Kanamori[26,27], Allen and Cahn[28], Sanchez and de Fontaine[29], Finel[30] and others have determined ground states of order on fcc and bcc lattices for first and second neighbor (also higher neighbor and multiplet) interactions. Given a set of V_r (or E_α), and c, the problem reduces to that of minimizing the internal energy (38) subject to constraints. Since (38) is linear in the pair correlation functions ξ_r, the problem can be handled by techniques of linear programming, the constraints being derived from Eq. (17), for instance, by noting that the cluster concentrations are non negative:

$$\sum_{\alpha \subseteq \beta} \Phi_\alpha(\sigma\beta)\ \xi^*_\alpha \geq -1 \quad . \qquad (58)$$

In principle, the minimization returns 0°K equilibrium values ξ^*_α of the correlation functions which uniquely determine the ground state structures to be expected under the specified conditions. In practice, the mathematical technique just described sometimes produces "non-constructible" structures. Nevertheless, in most cases, maps in V_r-parameter space are produced which indicate, for simple

stoichiometries, which ordered superstructures should be the stable ones for the chosen lattice (of the disordered state). Most commonly observed fcc and bcc-based ordered superstructures can be predicted by this analysis.

Since the EPI can be correlated with electronic parameters, the V_r maps can be transformed into structure maps in $\bar{N}_d$, δ_d, δ_{nd} space[25]. Predictions for paramagnetic transition metal alloys agree remarkably well with experiment. In a very recent study[31], ordering maps were also successfully derived on the basis of calculations simply involving a rectangular band approximation to the electronic DOS.

7. Construction of Phase Diagrams

The determination of ordered superstructures is an essential first step in the construction of temperature-concentration phase diagrams. Indeed, in the minimization of the free energy, it is essential to limit the set of cluster variables ξ_α: the members of the set are determined by the symmetry operations of the ordered ground state considered. Thus, given the range of EPI envisaged, to each disordered state lattice (α, say), corresponds a set of ordered superstructures $\{\alpha',\alpha'',\ldots\}$. Then at each temperature T and concentration c, the equilibrium correlations ξ^* are determined by Eqs. (28), the chemical potential difference $\mu_B-\mu_A$ is determined and the grand potentials

$$\Omega^\alpha = (F - N\mu\xi_s)^\alpha \qquad (59)$$

are calculated, where ξ_s is a normalized sum of point correlations over distinct sublattices. The free energy F in Eq. (59) is the sum E_{dis} plus E_{ord} minus T times the CVM configurational entropy, appearing as the second term of Eq. (30). The same procedure is repeated for other lattices and corresponding ordered superstructures $(\beta,\beta',\beta'',\ldots)$ and grand potentials Ω^α, $\Omega^{\alpha'}$, Ω^β,... are compared at each temperature. Intersections of two $\Omega(\mu)$ curves denote phase equilibrium between the two structures. The lowest lying Ω curve between intersections determines which phase is expected to be the equilibrium one. Grand potential diagrams are then converted to phase diagrams in (c-T) space by computing the concentrations corresponding to the equilibrium ξ^* obtained from Eqs. (28) for the equilibrium structures.

Other correlation functions determine, at equilibrium, expected cluster concentrations by use of Eqs. (17), hence a measure of SRO can be obtained. Long range order parameters are generally defined as appropriate linear combinations of point correlations ξ_i on the relevant sublattices.

This phase diagram construction is illustrated in the flow chart of Fig. 2. Only the tight binding TB portion has been implemented (top right hand side of Figure), not the KKR portion (left hand side). Satellite boxes indicate schematically possible experimental verification.

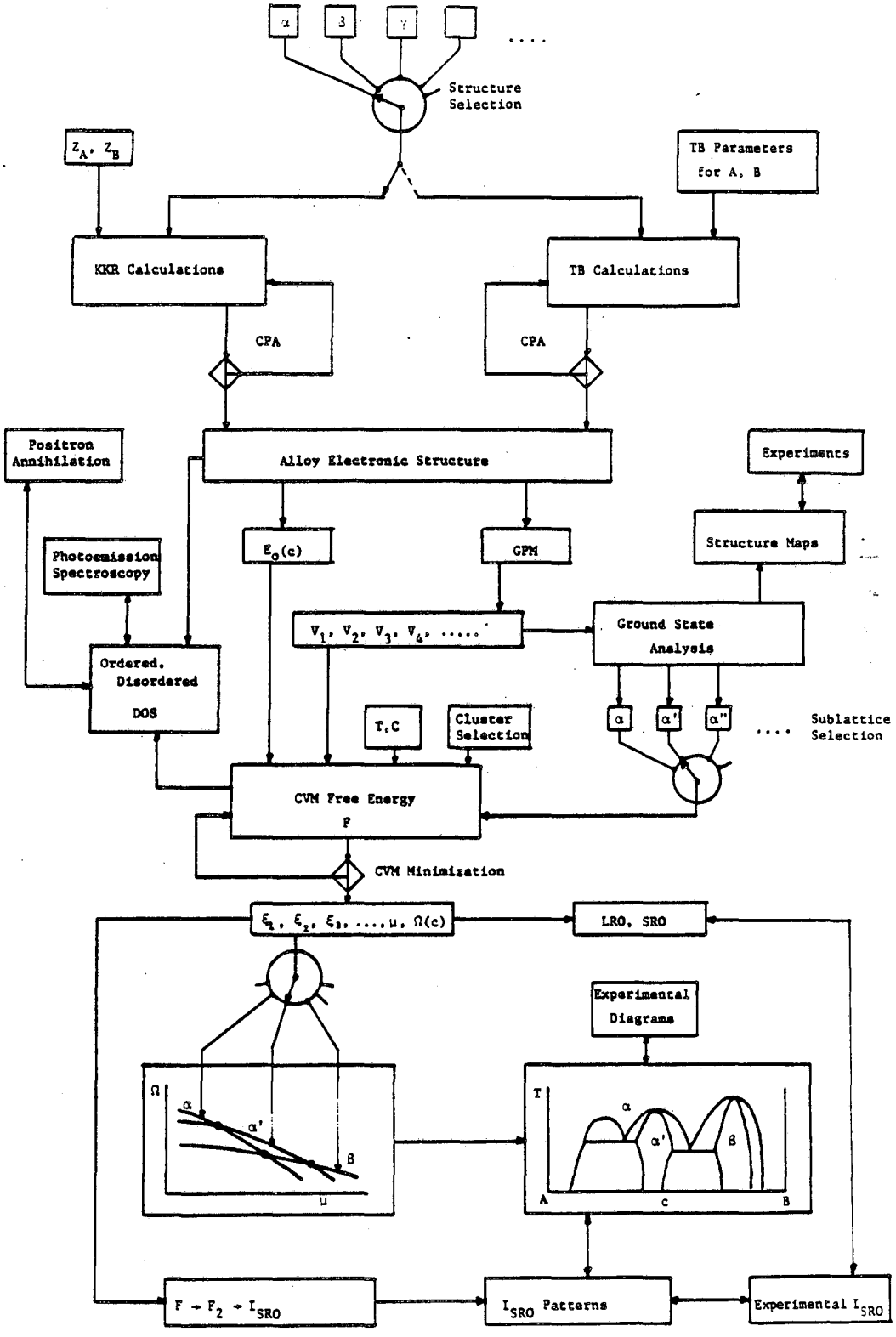

Fig. 2. Flow chart for phase diagram calculations.

8. Prototype Diagrams

As an illustration of the procedures outlined above, it was decided to perform some simple prototype phase diagram calculations involving the fcc lattice and its simplest ordered superstructures. Normally, the first nearest neighbor (nn) EPI, V_1, is expected to be the dominant one in the fcc case, so that the calculation of ΔE_{ord} will be limited to that nn contribution only. It follows from ground state analysis that, with $V_1>0$ (ordering case), the only ordered superstructures expected are the $L1_2$ (Cu_3Au-type) and $L1_0$ (CuAuI). For the purpose of performing sample calculations, "canonical" Slater-Koster parameters were used[21,22]: $dd\sigma=-1.385$, $dd\pi=\frac{1}{4}|dd\sigma|$, $dd\delta=0$. Charge transfer is expected to alter the values of the pure element d-band centers of gravity ε_A and ε_B in the alloy. Therefore, since charge transfer was not calculated, the diagonal disorder δ_d was regarded as a variable parameter, whose influence on the phase diagram is to be studied systematically. Values of $\delta_d=1.0$, 0.8 and 0.6 were chosen[22]. Results of energy calculations were expressed in canonical units (cu); if an average band width of ~5eV is taken, then 1cu≅4.5eV. This value was used to convert "canonical degrees" in the calculated phase diagrams to degrees absolute.

By convention, δ_d was taken to be positive: $\varepsilon_B>\varepsilon_A$. Therefore, we must necessarily have $N_A>N_B$, i.e., A and B belong to the end and the beginning of the transition metal series, respectively. The following pairs of numbers for d-band occupancy in the pure elements were selected: (9,3), (7,3) and (9,4), the first number being the value N_A, the second N_B. Since it was assumed that the number of s-electrons per atom in the solid was equal to one all across the transition metal series, the numbers N_A and N_B are simply one less than the group number in the Periodic Table.

Values of the energy of mixing ΔE_{dis} for the completely disordered state were obtained by subtracting the straight line interpolation between E_A and E_B from the values $E_{dis}(c)$ calculated by the procedures described above for the three (N_B, N_A) pairs of values and the three δ_d selected. Next, the concentration dependent EPI $V_1(c)$ were calculated, by Eq. (53), for the same set of electronic structure parameters. Results are displayed in Fig. 3, in canonical units. As expected[21,22], the $V_1(c)$ curves peak towards the center of the concentration axis whenever $\frac{1}{2}(N_A+N_B)\cong 5$ (half-filled alloy d-band), and towards the element with highest d-electron concentration for average band filling greater than 5. It is also seen in Fig. 3 that the amplitude of the $V_1(c)$ profile increases with increasing values of δ_d. These results are expected to hold quite generally, and influence very significantly the shape of the phase diagrams.

Several fcc-based phase diagrams have been calculated based on the results of Fig. 3[21,22]. Here, only the case $N_A=9$, $N_B=3$, $\delta_d=1.0$ will be presented (full curve for $V_1(c)$ in Fig. 3). The resulting phase diagram is shown in Fig. 4. The diagram

shows wide α (fcc) solid solubility, and three ordered phase regions: two of $L1_2$-type (α') with first-order transition temperatures, high for A_3B, low for AB_3, at roughly stoichiometric concentrations, and an $L1_0$ ordered phase region appearing by peritectoid reaction around the center of the phase diagram (α''). A prominent, and unexpected feature of the phase diagram is the presence of a narrow miscibility gap, persisting to very high temperatures, between two disordered solid solutions of different average compositions. The transitions temperatures are, of course, extremely high. This simply means that, with δ_d=0.1, melting would ocur before disordering could take place. Dashed curves in Fig. 4 refer to inherent "ordering" and "clustering" instabilities or spinodals[3].

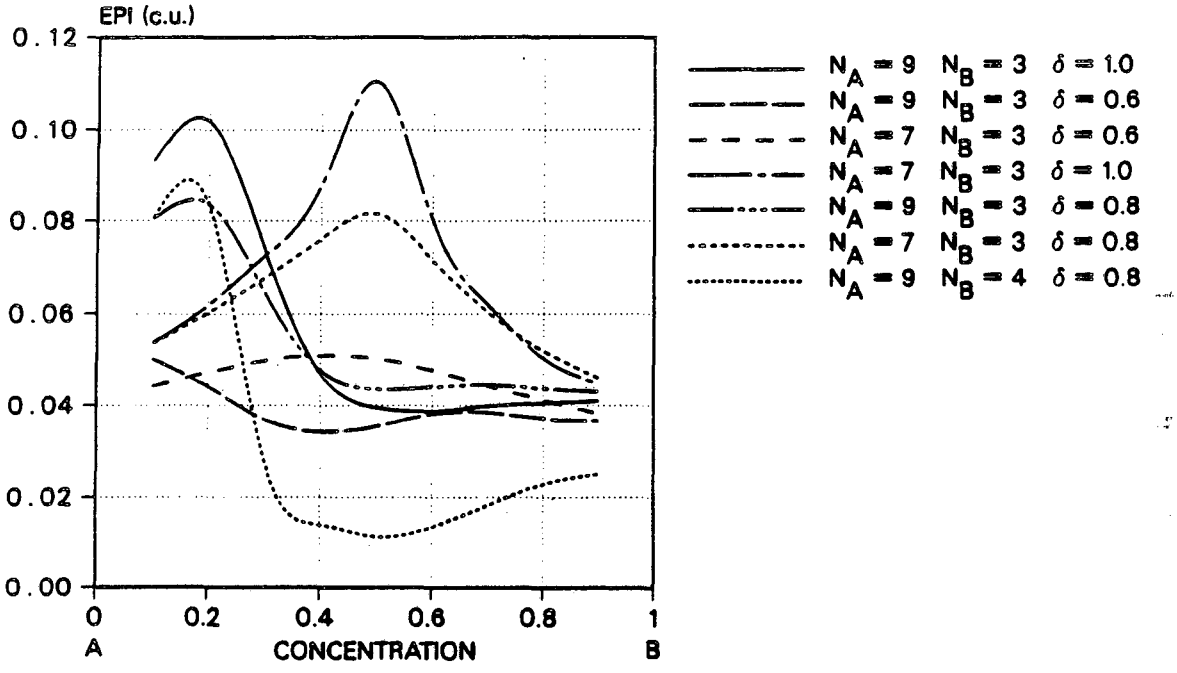

Fig. 3. Effective pair interaction V_1 (in canonical units) as a function of concentration for the indicated values of electronic parameters.

It is instructive to examine the various component curves of the total free energy, at given temperature, as a function of concentration. Figure 5 shows the "mixing" curves ΔE_{dis}, ΔE_{ord}, $-T\Delta S$ and the sum total ΔF at 1700K for the case depicted in Fig. 4. The full curves are for the disordered (α) phase and the dashed curve for the α' ($L1_2$) phase, the only ordered phase stable at this temperature. It is seen that the ΔE_{dis} curve, which is temperature independent, already contains a shallow concave region. This means that a common tangent can always be constructed to the ΔF curves except at extremely high temperatures where the convex $T\Delta S$ contribution is expected to dominate. The ΔE_{ord} contribution enhances the concavity, as seen in Fig. 5. Also of interest is the fact that the configurational entropy in the ordered state tends to zero at the A_3B stoichiometry, as expected.

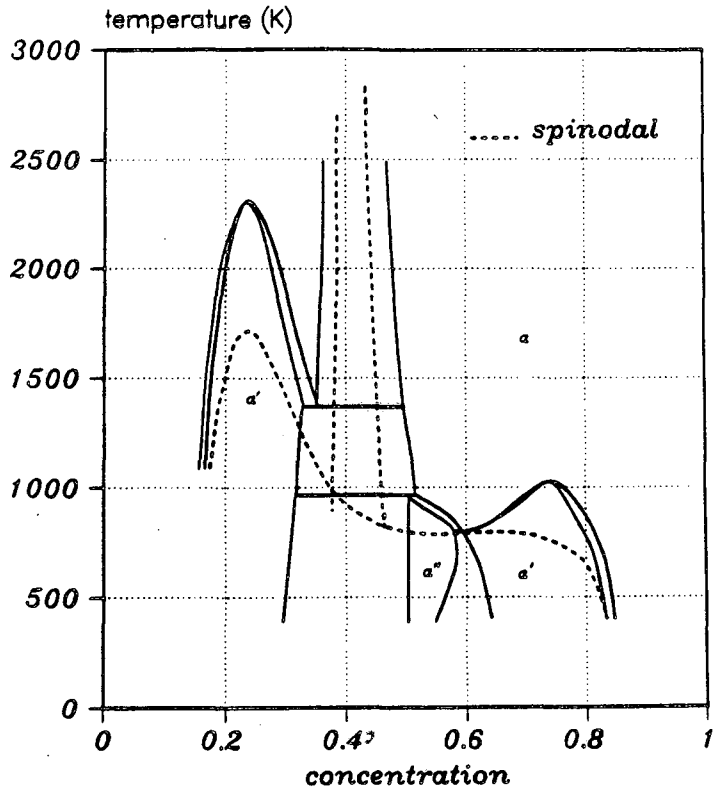

Fig. 4. Prototype phase diagram for N_A=9, N_B=3, δ_d=1.0. Phase α is the fcc solid solution, α' and α'' are $L1_2$ and $L1_0$ ordered superstructures, respectively.

The phase diagram shown in Fig. 5 thus illustrates that, in a purely "ordering" system (V_1>0 for all c), a very persistent miscibility gap (MG) can appear due to the intrinsic variation of thermodynamic parameters with concentration, not through any inherent "clustering" tendency associated with negative EPI. These extraneous MG tend to disappear as the diagonal disorder decreases. Presumably, charge transfer will attenuate the tendency towards phase separation in "ordering" systems.

9. Conclusion

The calculation of phase diagrams from first principles constitutes a very critical test of accuracy of both quantum and statistical mechanical models. The theoretical problems are extremely challenging and the expected results of considerable practical interest.

On performing the calculations, it becomes evident that the slightest variation of calculated energies can result in drastic changes in the topology of phase diagrams: the location of phase boundaries and even the nature of the phases in mutual

equilibrium is determined by the common tangent construction so that small alterations in the shape or relative positions of free energy curves can cause commong tangents to connect completely different sets of phases, structures, concentrations. In other words, phase diagrams result from "non-local minimization:" all possible free energy curves of all possible phases must be considered, at all concentrations, and compared to one another.

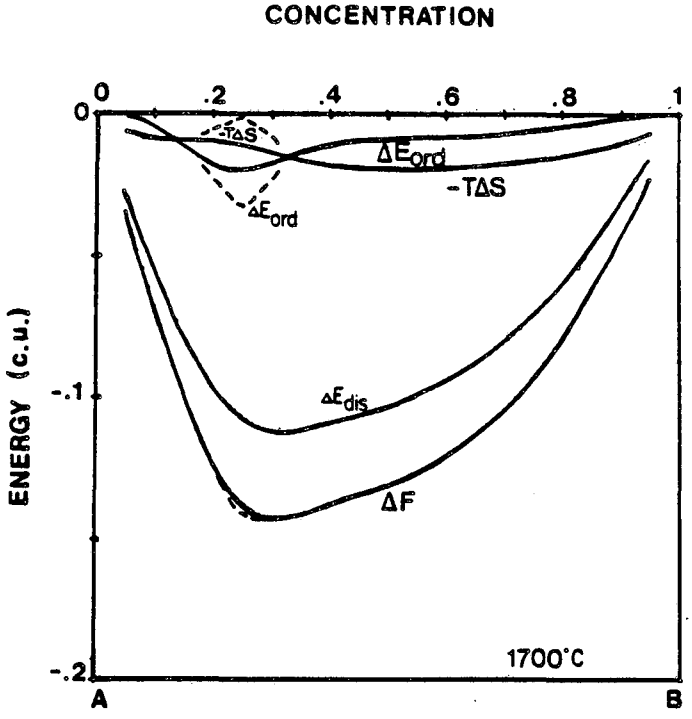

Fig. 5. Component curves of $\Delta F = \Delta E_{dis} + \Delta E_{ord} - TS$ for the phase diagram of Fig. 4 at 1700K; full lines: solid solution α, dashed lines: ordered phase α''.

Whether or not sufficient accuracy can be attained to reproduce experimental diagrams remains to be seen. In the present study, only "prototype" systems were considered. The tight binding CPA was used as basic quantum mechanical framework, and the CVM was used for the statistical mechanical calculations. Both models can be improved. In particular, it should be possible to take charge transfer and off-diagonal disorder into account. Furthermore, hopping integrals should be chosen that correspond to real systems to be modeled. Structures other than the fcc lattice and its simplest superstructures should be considered. In a very recent study, both fcc and bcc lattices and corresponding ground states were incorporated in the model, with the result that a reasonable approximation of the Ti-Rh phase diagram was calculated, including some experimentally observed metastable phases[32].

An extended version of the methods outlined here was developed by Sigli and Sanchez[23], with the result that very good quantitative agreement was obtained for the miscibility gap in the W-Cr system. Remarkable agreement was also obtained with available experimental data for the enthalpy of mixing of other transition metal bcc binaries.

Ultimately, it will be necessary to take vibrational entropy and elastic interactions into account. Perhaps the KKR-CPA will have to be brought into play for accurate truly first-principles calculations. Clearly, much remains to be done.

Acknowledgements

The author has benefitted from many discussions with colleagues and present and former students, among them: F. Ducastelle, F. Gautier, A. Gonis, A. Finel, B. L. Györffy, L. M. Falicov, J. M. Sanchez, C. Sigli, M. Sluiter, G. M. Stocks and P. Turchi. Calculations on prototype phase diagrams were performed by P. Turchi and M. Sluiter with partial support from a Grant from the Lawrence Livermore National Lab. This work was supported by the Director, Office of Energy Research, Office of Basic Energy Sciences, Materials Sciences Division of the U. S. Department of Energy under Contract Number DE-AC03-76SF00098.

References

1. J. S. Faulkner, "The Modern Theory of Alloys," in *Progress in Materials Science*, J. W Christian, P. Haasen and T. B. Massalski, Eds., Vol. 27, pp. 1-87, Pergamon Press (1982).

2. T. Mohri, J. M. Sanchez and D. de Fontaine, *Acta Metall.*, 33, 1171 (1985).

3. D. de Fontaine, "Configurational Thermodynamics of Solid Solutions," in *Solid State Phys.*, H. Ehrenreich, F. Seitz and D. Turnbull, Eds., Vol. 34, pp. 73-294, Academic Press (1979).

4. D. de Fontaine, in *Modulated Structure Materials*, NATO ASI Series E, No. 83, T. Tsakalakos, Ed. pp. 43-80, Martinus Nijhoff (1984).

5. D. de Fontaine, in *High-Temperature Ordered Intermetallic Compounds*, C. C. Koch, C. T. Liu and M. S. Stoloff, Eds., Materials Res. Soc. Symposium Proc. Vol. 39, pp. 43-64 (1985).

6. R. Kikuchi, *Phys. Rev.* **81**, 988 (1951).

7. J. M. Sanchez, F. Ducastelle and D. Gratias, *Physica (Amsterdam)*, **128A**, 334 (1984).

8. J. M. Sanchez and D. de Fontaine, *Phys. Rev. B*, **21**, 216 (1980).

9. T. Morita, *J. Phys. Soc. Jpn.* **12**, 753, 1060 (1957); *J. Math. Phys.* **13**, 115 (1972).

10. J. A. Barker, *Proc. Roy. Soc.*, **A216**, 45 (1953).

11. J. Hijmans and J. De Boer, *Physica* **21**, 471, 485, 499 (1967).

12. F. Ducastelle, *J. Phys. C* **8**, 3297 (1975).

13. F. Ducastelle and F. Gautier, *J. Phys. F* **6**, 2039 (1976).

14. C. Sigli and J. M. Sanchez, *CALPHAD* 8, 221 (1984).

15. A. Gonis, G. M. Stocks, W. H. Butler and H. Winter, *Phys. Rev. B*, 29, 555 (1984).

16. A. Bieber, F. Gautier, G. Treglia and F. Ducastelle, *Sol. St. Comm.*, 39, 149 (1981).

17. P. Turchi, G. M. Stocks and A. Gonis (private communication).

18. J. C. Slater and G. F. Koster, *Phys. Rev.* 94, 1498 (1954).

19. R. Haydock, in *Solid State Phys.*, H. Ehrenreich, F. Seitz and D. Turnbull, Eds., Vol. 35, pp. 215-294 (1980).

20. P. Turchi, F. Ducastelle and G. Treglia, *J. Phys.* C15, 2891 (1982).

21. P. Turchi, *Thèse de Doctorat d'Etat es Sciences Physiques*, Univ. Pierre et Marie Curie, Paris VI (1984).

22. P. Turchi, M. Sluiter and D. de Fontaine (to be published).

23. C. Sigli, *Ph.D. Thesis*, Columbia University, NY (1986).

24. B. Velicky, S. Kirkpatrick and H. Ehrenreich, *Phys. Rev.* 175, 747 (1968).

25. A. Bieber and F. Gautier, *Acta Metall.* (in press).

26. J. Kanamori, *Progs. Theor. Phys. (Japan)* 31, 66 (1966).

27. J. Kanamori and Y. Kakehashi, *J. Phys. (Paris)* 38, C7-274 (1977).

28. S. M. Allen and J. W. Cahn, *Acta Metall.* 20, 423 (1972); *Scripta Metall.* 7, 1261 (1973).

29. J. M. Sanchez and D. de Fontaine in *Structure and Bonding in Crystals*, M. O'Keeffe and A. Navrotsky, Eds., Vol. II, pp. 117-132, Academic, NY (1981).

30. A. Finel (private communication).

31. M. Sluiter, P. Turchi and D. de Fontaine (to be published).

32. M. Sluiter, P. Turchi, Zehzong Fu and D. de Fontaine (to be published).

LAWRENCE BERKELEY LABORATORY
TECHNICAL INFORMATION DEPARTMENT
UNIVERSITY OF CALIFORNIA
BERKELEY, CALIFORNIA 94720